MORPHOLOGY OF HDPE/PET/E-GMA BLENDS.
STUDY OF THE MECHANISM FOR TOUGHENING WITHOUT RIGIDITY LOSS

CIRO FEREGRINO MONTES

SILVIO ALBERTO OSPINA SALGADO

Plásticos Técnicos Mexicanos S.A. de C.V.
Carretera México-Tequisquiapan Km 3.0, Zona industrial Valle de Oro, 76803
San Juan del Río, Querétaro, México

Instituto de Capacitación e Investigación del Plástico y del Caucho, ICIPC
Universidad Eafit - Carrera 49 # 5 Sur 190, Bloque 37
Medellín, Antioquia, Colombia

2020

ACKNOWLEDGMENT

I gratefully acknowledge Plásticos Técnicos Mexicanos S.A. de C.V., CINVESTAV unidad Querétaro and ICIPC for the provided support, material and laboratory equipment.

To my mentors, MSc. Silvio Ospina and MEng. MSc. Ricardo Peña, thank you for sharing your knowledge and experience, for your advices and your unconditional support.

To my consultants, Ph.D Mauricio Vasquez and Ph.D Alejandro Manzano, I am truly grateful to you for giving me inputs and suggestions that greatly improved this work.

To my team: Daniel, Hermes and Nallely. Thank you for all your help in this process.

And finally, to my whole family. Thank you for all the support and encouragement during all this time. I love you and I owe all to you.

CONTENIDO

Pag.

ABSTRACT

The morphology of HDPE/PET/E-GMA ternary blends showing toughening without rigidity loss was studied as a response to the need for improve the mechanical properties of recycled materials in an upcycling context. Izod impact test, flexural properties, SEM observation, DSC, DMA and rotational rheometry techniques were used in this work. The morphology formation mechanism proposed in this work assumes that there is high miscibility of E-GMA on HDPE; therefore, E-GMA alone does not improve the impact strength of HDPE, but with the addition of PET the E-GMA surround the droplets of dispersed phase seeking to react and forms a core shell morphology.

INTRODUCTION

Circular Economy (CE) is gaining global momentum. Its core idea of moving away from the current linear 'take-make-use-dispose' economy to one that is restorative and regenerative by design has been embraced by governments around the world. CE is "a system that has the ability to restore, retain and redistribute materials, components and products (MCPs) in the best possible way and for as long as it is environmentally, technically, socially and economically feasible". This stipulates a fundamental reconsideration of resource producing, consuming and recovering (Hahladakis & Iacovidou, 2019).

Current approaches to increasing resource efficiency focus on recycling and a Circular Economy. This can be effective when materials are truly recycled, as opposed to down-cycled with a related loss in material quality, material purity and material value (Bridgens et al, 2018).

Today, recycling is considered as one of the best options in the solid waste management hierarchy to reduce the impacts presented by end of life (EoL) and end of use (EoU) post-consumer packaging plastic wastes. Other than contributing to municipal solid waste management by diverting materials which have economic value from the main waste flow, thus reducing quantities of waste to be collected and disposed, recycling provides the opportunity to use recovered plastics to manufacture a new product. For these reasons, recycling provides opportunities for recovered polymers to cascade through multiple stages throughout their lives hence contributing to sustainable manufacturing (Mwanza & Mbohwa, 2017).

It is known by those who integrate the polymeric material recycling industry that there is a loss in the molecular weight of the resin, with the corresponding effect on the mechanical properties, each time the product ends its life cycle due primarily to the degradation caused by exposure to environmental factors and high temperatures in

oxidizing atmosphere during the transformation process. Owing to this, the percentage of use of recycled material is limited for the same application or it is used in products with lower mechanical performance as opposed to the upcycling concept. Upcycling is a term from 1990s, which means “reuse (discarded objects or material) in such a way as to create a product of higher quality or value than the original” (Bridgens et al, 2018).

In municipal solid waste around the world, plastics account for an increasing fraction, and solid household waste is made up of a mixture of largely polyolefin-based plastics, such as high-density polyethylene (HDPE), low density polyethylene (LDPE), polypropylene (PP), and poly (ethylene terephthalate) (PET) (Lei, Wu & Zhang, 2009).

PE and PP make up well over half of the more than 150 million metric tons of thermoplastics demanded worldwide, with PE accounting for nearly two-thirds of all polyolefins used. This consumption is roughly equivalent to 15 kg of polyolefin product per year for each person on earth. And this usage will grow; worldwide PE production alone is expected to rise from about 80 million metric tons in 2013 to around 120 million in 2023 (over a 4% annual increase). So, given this demand for polyolefins and the range of product types available with these versatile materials, it is likely that most people in the world now come into contact with an article made from PE or PP at least once each day (Tolinski, 2015).

PE and PP have traditionally been categorized as ‘commodity plastics’ due to their low cost, this is misleading; in fact, polyolefins have been used for some engineering applications for years. Their properties continue to be improved by the use of additives for using them in applications with better mechanical performance (Tolinski, 2015).

Polyethylene terephthalate (PET) is a polymer that has great importance among the plastics in the world. Its thermoplastic recyclability makes it a first choice for various applications. Its properties, uses and industrial innovations that increases its

consumers demand result in tons of its scrap creation in the environment. Its toughness, resilience non-degradable nature that makes its waste increases over years constitutes hazard to environment when dumped after use, cause serious problems to the environs and called for its recycling. PET waste accounts for 8% by weight and 12% by volume of the world's solid waste with volumetric increment at alarming rate (Raheem et al, 2019).

PET and HDPE are used extensively in packaging materials, and their annual rates of consumption steadily increase. It has been shown that HDPE/PET blends are less brittle than PET, do not need to be dried before processing, and are stiffer, better flowing, and faster cooling than HDPE (Lei, Wu & Zhang, 2009).

Studies of PET/HDPE blends mainly focus on improving compatibility of PET and HDPE since they are inherently incompatible due to the great difference in solubility parameters between them. PET/HDPE blends have been compatibilized with elastomers and functionalized elastomers, functional group grafted polyolefins, vinyl acetate based copolymers, and reactive monomers (Lei, Wu & Zhang, 2009).

The key issues for the production of high-performance immiscible polymer blend cover the following aspects: (i) Homogeneous dispersion and embedding of dispersed phase in matrix; (ii) strong interfacial interaction between the dispersed phase and matrix; and (iii) adequate morphology design for dispersed phase and matrix (Wang et al, 2018).

The phase morphology is generally determined by the following factors: material characteristics (interfacial tension, melt-viscosity, melt-elasticity, and molecular weight) and processing parameters (time of mixing, temperature of mixing, screw speed, mixer type). Likewise, the morphology of polymer blends is influenced both by the thermodynamic and kinetic factors (Shen et al, 2015).

The dispersed phase can possess different morphologies, such as spherical drop, cylinder, fiber, sheet, or co-continuous phase. The resulting morphology is partly

determined by processing conditions (external fields such as temperature and pressure) (Wang et al, 2018).

Some authors have demonstrated that ternary blends comprising HDPE, PET and E-GMA can improve the impact strength of the matrix (Lei et al, 2009; Salleh et al, 2013 y Kalfoglou et al, 1995), even Lei, Wu & Zhang (2009) developed microfibrilar composites with this formulation, but not efforts have been done to deep study the phenomena around this behavior.

A core shell morphology has been proposed to improve toughness with little rigidity loss in immiscible blend PP/HDPE/EPR (Jia et al, 2019), introducing the concept of 'equivalent rubber content and the criterion of 'critical interparticle distance' on the basis of percolation of stress volumes. Several authors have studied ternary blends using this core shell morphology approach explaining the mechanical behavior of them. The main aspect in core shell morphology the main aspect that defines a core shell morphology is the existence of three phases, matrix, core and shell (Jia et al, 2019; Chen et al, 2015; Khalili et al, 2014; Mi et al, 2019; Luzinov et al, 2000).

Palierne (1990) considered the linear viscoelastic behavior of concentrated emulsions of incompressible viscoelastic materials in the presence of an interfacial agent. He worked out a linear viscoelastic constitutive equation for the emulsion as a function of the linear viscoelastic behavior of the phases, the aim distribution of the dispersed droplet, and the interfacial tension. Graebling et al (1993) estimated the interfacial tension from viscoelastic data on binary blends.

Several authors used Harkin's equation in which two distinct phases are dispersed in a matrix phase to predict the morphology of ternary blends (Shen et al, 2015). For a ternary blend system supposing A as the matrix and B and C as the dispersed phases the spreading coefficient λ_{BC} of the B - phase on the C - phase is:

$$\lambda_{BC} = \gamma_{AC} - \gamma_{AB} - \gamma_{BC} \quad (1)$$

Where λ_{ij} is the spreading coefficient of i over j and γ_{ij} is the interfacial tension between i and j. In the case, B encapsulated by C, λ_{BC} must be positive. Similar treatment gives the spreading coefficient of the C-phase on the B-phase:

$$\lambda_{CB} = \gamma_{AB} - \gamma_{AC} - \gamma_{BC} \quad (2)$$

In the case when both λ_{CB} and λ_{BC} are negative, B and C will tend to form separated phases. For a given matrix, there are four possible types of morphologies:

Fig 1. Some of the most common morphologies observed in ternary blends

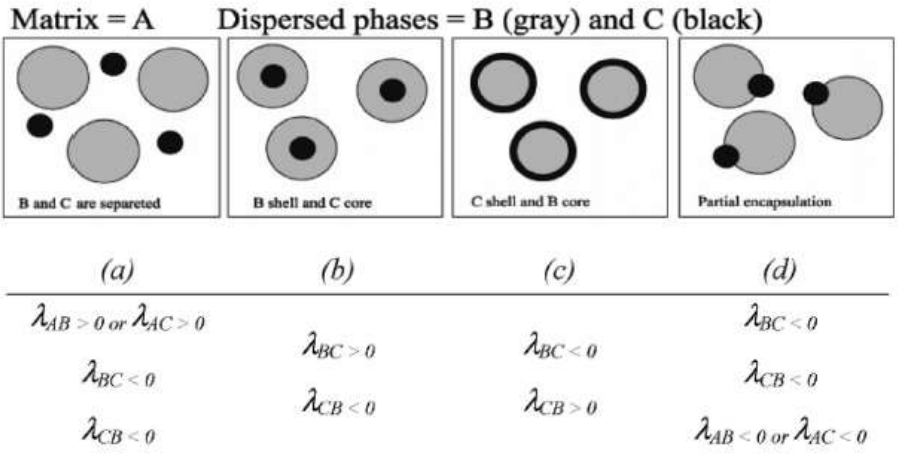

Fuente: Shen et al, 2015

According to Shen et al (2015), Gramespacher and Meissner discovered that the relaxation spectra of blends could be considered as the sum of each phase's relaxation spectra. According this finding and Choi and Scholwalter's research based on the empirical rule of blending, they proposed a series of equations (eqs. (3) and (4)) to calculate storage and the loss moduli of blends. These equations allowed one to describe the influence of the interfacial tension on the storage and the loss moduli in a broad frequency range for all mixing ratios of the blend components. Moreover,

the weighted relaxation spectra of blends show an additional peak with a characteristic relaxation time that is correlated with the interfacial tension (eqs. (5)-(8)). With these equations, it is possible to calculate the interfacial tensions between two phases when it is known the characteristic relaxation time of blends shear oscillations.

$$G'(\omega) = \eta \frac{\omega^2(\tau_1-\tau_2)}{1+\omega^2\tau_1^2} = \frac{\eta}{\tau_1}(1-\frac{\tau_2}{\tau_1})\frac{\omega^2\tau_1^2}{1+\omega^2\tau_1^2} \quad (3)$$

$$G''(\omega) = \eta \frac{(\omega^3\tau_1\tau_2-\omega)}{1+\omega^2\tau_1^2} = \frac{\eta}{\tau_1}\left(1-\frac{\tau_2}{\tau_1}\right)\frac{\omega^2\tau_1}{1+\omega^2\tau_1^2} = \omega\eta\frac{\tau_2}{\tau_1} \quad (4)$$

Where,

$$\eta = \eta_m[1+\phi\frac{(5K+2)}{2(K+1)}+\phi^2\frac{5(5K+2)^2}{8(K+1)^2}] \quad (5)$$

$$\tau_1 = \tau_0[1+\phi\frac{5(19K+16)}{4(K+1)(2K+3)}] \quad (6)$$

$$\tau_2 = \tau_0[1+\phi\frac{3(19K+16)}{4(K+1)(2K+3)}] \quad (7)$$

$$\tau_0 = \frac{\eta_m R}{\gamma}\frac{(19K+16)(2K+3)}{40(K+1)} \quad (8)$$

Where, η, η_d and η_m are the Newtonian viscosity of blends, dispersed phase and matrix; K= η_d/η_m ; γ is the interfacial tension; φ is the volume fraction of dispersed phase; R is the radius of dispersed phase; τ_0 is the characteristic relaxation time of interphase; τ_1 is the characteristic relaxation time of dispersed phase.

Plásticos Técnicos Mexicanos S.A. de C.V. (PTM) is a plastic manufacturing company specialized in material´s handling products. Since 1976 PTM has produced plastic parts, reaching 33 000 tonnes of processed resin in 2019. The commitment to the use of recovered materials based on an upcycling vision has allowed us to incorporate up to 100% of recycled materials in some of our products. This vision leads us to look for new sources of recovered material, with the best mechanical properties, that allow us to have an advantage against our competitors

The aim of this work is to study the morphology and behavior of HDPE / PET mixtures compatible with E-GMA for the understanding of the phenomena that cause an increase in the mechanical properties of the HDPE matrix. This will allow the study to be transferred to recovered materials and finally to design materials, with an upcycling perspective, with better properties that allow us to have products of greater specifications

1. EXPERIMENTAL SECTION

1.1 Materials

Commercial grade HDPE (PADMEX 65080, MFI=8.0 g/10 min @ 190 °C 2.16 Kg, Petroleos Mexicanos, México), PET (Eastlon PET CB-606, IV= 0.83 dl/g, Far Eastern New Century, Taiwan) and E-GMA copolymer (Lotader AX8840, MFI=5.0 g/10 min @ 190 °C 2.16 Kg, Arkema, France) were used in this work to analyze its individual properties, prepare binary blends (HDPE/PET 95%/5% w/w, HDPE/E-GMA 95%/5% w/w, PET/E-GMA 95%/5% w/w) and to prepare ternary blends (HDPE/PET/E-GMA 85%/10%/5% w/w, HDPE/PET/E-GMA 75%/20%/5% w/w, HDPE/PET/E-GMA 65%/30%/5% w/w).

The decision to fix the concentration of E-GMA at 5% w/w and use PET only up to 30% w/w was based on the previous work reported for Salleh et al (2013) in which it is shown that using percentages above 5% of E-GMA does not provide benefit in mechanical properties and adding a percentage of PET greater than 30% reduce the impact strength of the blend.

1.2 Blend preparation

For the preparation of binary and ternary blends, the components were weighed at the designed mass ratio and blended in a Labtech Twin Screw extruder (LTE-2640, 26 mm diameter, L/D 40, OD/ID 1.3) at 280 °C (Flat profile) and 800 RPM. All the blends were produced at the same feed rate, 25 Kg/h. The screw configuration was the same for all the blends, it included distributive (30°, 60°) and dispersive (90°) mixing elements. A degassing vacuum zone at the end of the extruder was used to produce 30 cm Hg vac. In order to evacuate residual moisture. The PET was dried prior extrusion at 120 °C for 4 h in a Motan Bin S 15L drier.

1.3 Test specimen preparation

All the test specimen for Izod impact strength and flexural tests were injection molded in a 35 A Boy Machine using an Axxicon AIM Quick Change mold and an ISO type B insert. All the individual materials and blends were injected with the same parameters. The temperature profile was set to 250°C in the feeding zone and nozzle and 280 °C in the middle zone. Except for the temperature that was adjusted due to the PET content, all the injection molding parameters were defined according to the ISO 1872-2 standard. The mold temperature was 40 °C. The theoretical flow front velocity was 100 mm/s in the cross section of the test specimen, the specific hold pressure was set to 575 bar for 25 seconds, and additionally 10 second as cooling time were employed. The tangential velocity during plastification was 0.2 m/s. The cycle time was about 40s.

1.4 Impact strength test

The Izod impact tests were performed in a Tinius Olsen IT 504 pendulum according to ISO 180 with type A notch. The capacity of the pendulum was 2.8 J.

1.5 Flexural properties test

The flexural properties were measured in a Shimadzu AGS-X 5 universal testing machine according to ISO 178 at a 2mm/min test speed and a 64 mm span.

1.6 Scanning electron microscope observation (SEM)

SEM Micrographs were obtained in a JEOL JXA8530F electron microscope. Fractured specimens from impact test were polished and stained with a solution of foron blue E-BL in water at 1% for 24 h at 80 °C in order to reveal polar groups. After this, the samples were gold coated in order to increase its electric conductivity for SEM observation. The operating voltage was 20 KV. Additional micrographs of the binary HDPE/E-GMA and PET/E-GMA blends were obtained at the same conditions

but different preparation. The polished specimens were etched in n-heptane for 1 h at 70 °C. All the SEM micrographs were obtained at CINVESTAV (Centro de investigación y de estudios avanzados) Querétaro, México.

1.7 Differential scanning calorimetry measurement (DSC)

DSC tests were made according to ASTM D3418-15 on a TA instruments DSC Q200 calorimeter with 1 °C /100 s modulation. An inert nitrogen atmosphere (99.995%) was employed during the tests. The samples were heated from 25 to 280°C at a heating rate of 10 °C/min, then cooled at the same rate until 40°C and heated again until melting temperature. All DSC tests were performed at ICIPC (Instituto de capacitación e investigación del plástico y del caucho) Medellín, Colombia.

1.8 Dynamic mechanical analysis measurement (DMA)

A TA Instruments DMA 850 was used in dual cantilever mode. The HDPE, E-GMA and HDPE/PET/E-GMA (65/30/5) samples were heated from −60°C to melting point at a heating rate of 5 °C/min while the PET sample start temperature was 30 °C. The oscillatory frequency was 1 Hz and the amplitude was 35 μm.

Additional tests were performed for HDPE/PET/E-GMA (65/30/5) ternary blend, HDPE/E-GMA and PET/E-GMA binary blends in order to seek the E-GMA glass transition with higher resolution. For

this test the samples were heated from -20 °C to -5 °C, the heating rate was 1 °C/min, the oscillatory frequency was 100 Hz and the amplitude was maintained at 35 μm.

1.9 Rotational rheometric analysis

The rheometric analysis were performed on a TA instruments AR 2000 ex rheometer at 250 °C with parallel plates geometry and a sweep was made between 628 to 0.6 rad/s. This test was performed according to ISO 6721. All the rheometric analysis were performed at ICIPC (Instituto de capacitación e investigación del plástico y del caucho) Medellín, Colombia.

2. RESULTS AND DISCUSSION

2.1 Mechanical properties

Table 1. Mechanical properties of binary and ternary blends

	Impact Strength (KJ/m²)			Flexural Strength (MPa)			Flexural Modulus (MPa)		
	Value	σ	%Vs HDPE	Value	σ	%Vs HDPE	Value	σ	%Vs HDPE
HDPE	4.44 C	0.15		25.18	0.22		1136	36	
PET	2.62 C	0.05		79.93	0.26		2318	64	
HDPE/PET (95/5)	3.47 C	0.14	-21.85	26.22	0.36	4.13	1177	68	3.61
HDPE/E-GMA (95/5)	4.19 H	0.12	-5.63	23.6	0.3	-6.27	1094	76	-3.70
PET/E-GMA (95/5)	9.93 C	0.62		74.23	0.59		2282	62	
HDPE/PET/E-GMA (85/10/5)	4.72 H	0.28	6.31	26.28	0.59	4.37	1119	43	-1.50
HDPE/PET/E-GMA (75/20/5)	4.78 H	0.10	7.66	28.02	0.53	11.28	1214	39	6.87
HDPE/PET/E-GMA (65/30/5)	5.51 H	0.15	24.10	29.46	0.43	17.00	1231	38	8.36

PET/HDPE blends are inherently incompatible due to the great difference in solubility parameters between them [4], and we can see this behavior in the impact strength of the binary HDPE/PET blend which showed a 21.85% decrease against pristine HDPE. On the other hand, ternary HDPE/PET/E-GMA blends showed higher impact strength than pristine HDPE and the trend shows an improvement in this property by increasing the concentration of PET.

Traditionally, elastomeric (rubbery) polymers added to polyolefins could soften and toughen polyolefins for enhance impact strength, but at the cost of sacrificing rigidity expressed as flexural modulus (Tolinski, 2015). In this case with the ternary blends we are improving impact strength on HDPE and at the same time enhancing flexural properties. A similar behavior has been reported by Chen et al (2015) for PP/EPR/HDPE blends. According to them, this behavior can be attributed to a combination of toughening induced by the decrease of interparticle distance between EPR shell particles on the PP matrix and the premise of not increasing the actual rubber content and the rigidity contribution induced by the 'hard' HDPE core. Nevertheless, binary blend HDPE/E-GMA shows lower Impact strength than pristine HDPE which is an indicative than E-GMA does not operate like a conventional elastomeric impact modifier although it does decrease flexural properties. On the contrary, In PET/E-GMA binary blend E-GMA does improve PET impact strength with a decrease in the flexural properties, as it is supposed to do a conventional impact modifier.

2.2 Scanning electron microscope observation (SEM)

Fig 2. HDPE/PET (95/5) binary blend morphology

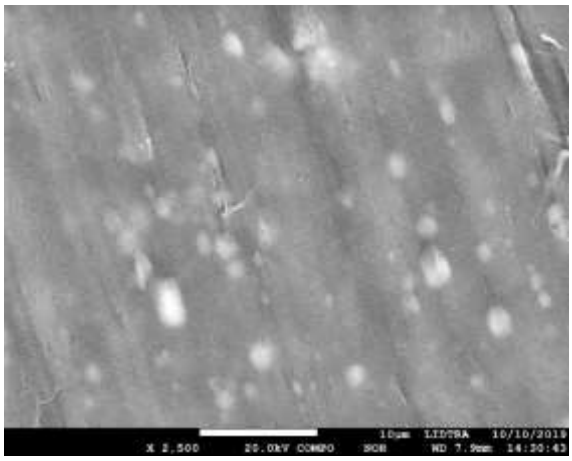

Fig 3. HDPE/PET/E-GMA (85/10/5) ternary blend morphology

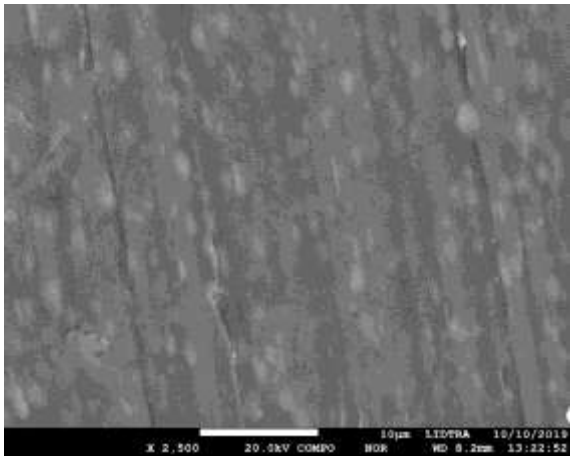

Fig 4. HDPE/PET/E-GMA (65/30/5) ternary blend morphology

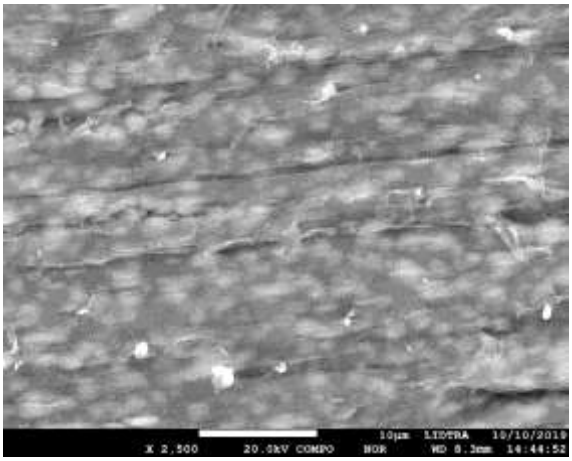

Table 2. Radius of dispersed phase on blends

Columna1	Radius of dispersed phase (μm)	σ
HDPE/PET (95/5)	0.825	0.38
HDPE/PET/E-GMA (85/10/5)	0.664	0.24
HDPE/PET/E-GMA (65/30/5)	0.744	0.34

Figs 2, 3 and 4 shows the morphology of HDPE/PET (95/5) binary blend, HDPE/PET/E-GMA (85/10/5) ternary blend morphology and HDPE/PET/E-GMA (65/30/5) ternary blend morphology respectively. It can be noticed a PET dispersed phase within an HDPE matrix. Table 2 shows the radius of dispersed phase and its standard deviation obtained from Figs 2, 3 and 4 using imageJ software. As can be seen, the addition of E-GMA in the HDPE/PET blends improve the dispersion and distribution of the PET dispersed phase within the HDPE matrix, this is showed by a smaller particle size, while the distribution can be seen directly from the micrographs. Additionally, the lower value for the standard deviation in the ternary blends is proof of better homogenization. Analyzing together the information provided by the mechanical properties and the SEM images it is possible to correlate the improvement in the impact strength between the HDPE/PET/E-GMA (65/30/5) against HDPE/PET/E-GMA (85/10/5) with the interparticle distance of the dispersed phase. However, due to the low impact strength of pure PET and the poor miscibility between HDPE and PET, PET itself has a little – or negative- toughening effect for HDPE as can be seen in HDPE/PET binary blend impact strength, while adding PET on HDPE/E-GMA blend the ternary blend exhibits an excellent toughness despite the fact E-GMA alone doesn´t improve HDPE properties. This fact shows that there is a synergistic effect between PET and E-GMA in toughening HDPE.

At this point, is it possible to propose two main possible toughening mechanisms in the ternary HDPE/PET/E-GMA blends: Core shell morphology with E-GMA working as a rubbery shell for a hard PET core or E-GMA works as a compatibilizer improving the interfacial adhesion between HDPE and PET.

2.3 Differential scanning calorimetry measurement (DSC)

DSC test results are displayed in Fig 5. As can be seen, the main melting transitions of PET and HDPE remain virtually unchanged comparing with HDPE/PET/E-GMA (65/30/5). According to ASTM D3418-15, this minimal displacement in the transition temperature can be attributed to the method´s repeatability. This suggests that in the ternary blend PET and HDPE remains as separated phases without the visible effect of E-GMA working as a conventional compatibilizer. The melting temperature of E-GMA was detected at 104.01 °C and is not possible to found in the ternary blend. There are two possible reasons for this, the E-GMA melting transition could be overlapped by the HDPE one or the influence of PET and HDPE is restricting E-GMA crystallization. According to Scheirs (2003), E-GMA reacts with PET through the mechanism in Fig 6. The addition of PET large chain segments seems to be a greater impediment for the crystallization of the E-GMA than the possible interaction with the HDPE.

Table 3. Enthalpy values obtained by DSC for pristine HDPE, PET, E-GMA and HDPE/PET/E-GMA ternary blend

	$\Delta Hm_{E\text{-}GMA}$	Theoretical	ΔHm_{HDPE}	Theoretical	ΔHc_{PET}	Theoretical	ΔHm_{PET}	Theoretical
PET	-	-	-	-	31.9	-	26.3	-
HDPE	-	-	230.5	-	-	-	-	-
E-GMA	81.83	-	-	-	-	-	-	-
HDPE/PET/E-GMA (65/30/5)	N/D	4.1	147.7	149.8	4.9	9.6	7.5	7.9

Table 3 shows the enthalpy values obtained by DSC for pristine HDPE, PET, E-GMA and HDPE/PET/E-GMA ternary blend. The theoretical enthalpy values that should appear in the ternary blend were calculated according to its weight composition and the enthalpy values of the pristine individual materials in order to evaluate the crystallization behavior of the ternary blend. PET shows a lower crystallization enthalpy than the theoretical one but the melting enthalpy matches well with the theoretical prediction, this suggests that the crystallization during the cooling stage was greater in the ternary blend than in pristine PET. For HDPE, the melting enthalpy matches very well with the predicted value, with the difference being so small that it can be attributed to the method´s repeatability. This fact discards the possibility that the improvement in mechanical properties shown by ternary blends is due to the effect of a change in the crystallinity of the HDPE matrix.

Fig 5. Second heating DSC thermogram of PET, HDPE, E-GMA and HDPE/PET/E-GMA (65/30/5) samples

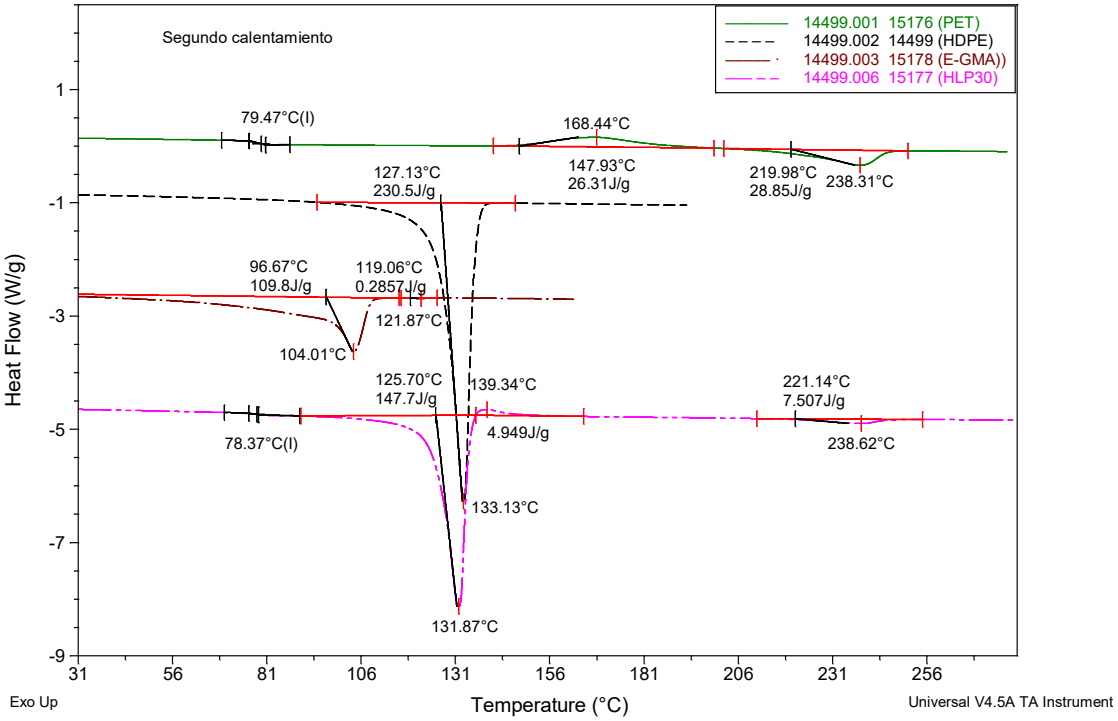

Fig 6. Reaction mechanism proposed by Scheirs

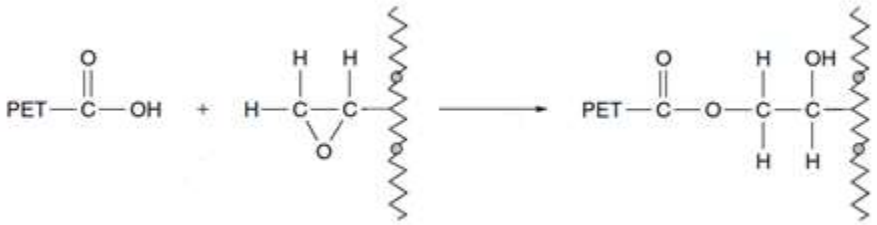

Fuente: Scheirs, 2003

2.4 Dynamic mechanical analysis measurement (DMA)

As it can be seen on fig 7 and table 4, the main α transition of PET is located at 83.2 °C, HDPE has its broad α relaxation centered around 51.3 °C and E-GMA presents its main transition at -13.6 °C. In the other hand, the HDPE/PET/E-GMA (65/30/5) ternary blend presents 2 transitions, one at 56.8 °C associated with the HDPE content and the second one at 82.5 °C relative to PET. At this test conditions it is not possible to observe in the HDPE/PET/E-GMA (65/30/5) ternary blend the transition associated to E-GMA. This fact, and the shift in the HDPE and PET transition temperatures towards each other suggests that E-GMA is only working as a compatibilizer helping in the dispersion of PET in the HDPE matrix and enhancing the interfacial interaction, giving as a result a compatibilized binary HDPE/PET blend.

Fig 7. DMA test results showing loss modulus Vs temperature for HDPE, PET, E-GMA and HDPE/PET/E-GMA (65/30/5) (heating rate 5 °C/min and oscillatory frequency 1 Hz)

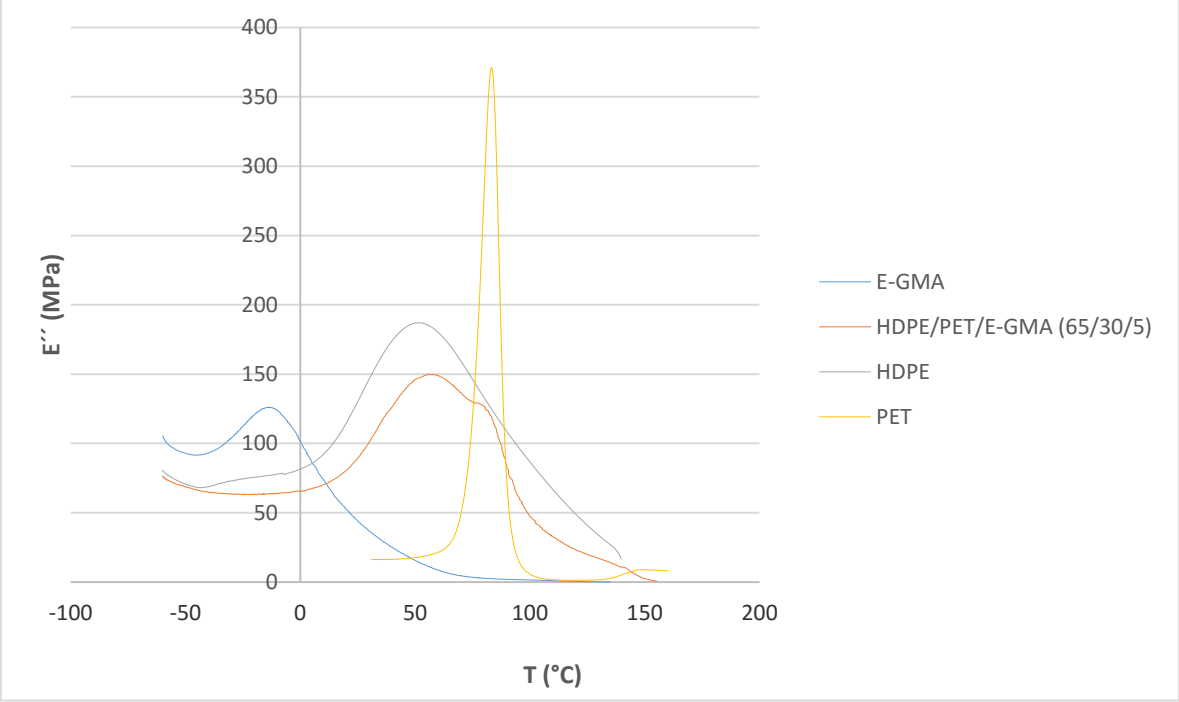

Table 4. Temperature at peak of E´´ in fig 6

Material	Temperature at peak (°C)
PET	83.2
HDPE	51.3
E-GMA	-13.6
HDPE/PET/E-GMA (65/30/5)	56.8
HDPE/PET/E-GMA (65/30/5)	82.5

Nevertheless, fig 8 and table 5 show the results of the DMA test for the loss modulus against temperature at higher frequency and lower heating rate for PET/E-GMA, HDPE/E-GMA and HDPE/PET/E-GMA (65/30/5) blends. At this test conditions, it is possible to see the transition associated with E-GMA in the ternary blend at -19.27 °C. This transition is shifted to a lower temperature compared with the previously obtained, but it is not possible to discern between associating this to the different test conditions or to miscibility with any of the other components of the blend. PET/E-GMA blend shows this transition associated with E-GMA at -11.96 °C while HDPE/E-GMA blend does not show this transition at the given temperature range, but its tendency gives rise to speculation about a possible peak at a lower temperature. These facts reinforce the possibility of high miscibility between HDPE and E-GMA, which is consistent with the fact that in the HDPE / E-GMA binary blend the E-GMA does not behave as rubbery impact modifier.

Fig 8. DMA test results showing loss modulus Vs temperature for PET/E-GMA, HDPE/E-GMA and HDPE/PET/E-GMA (65/30/5) (heating rate 1 °C/min and oscillatory frequency 100 Hz)

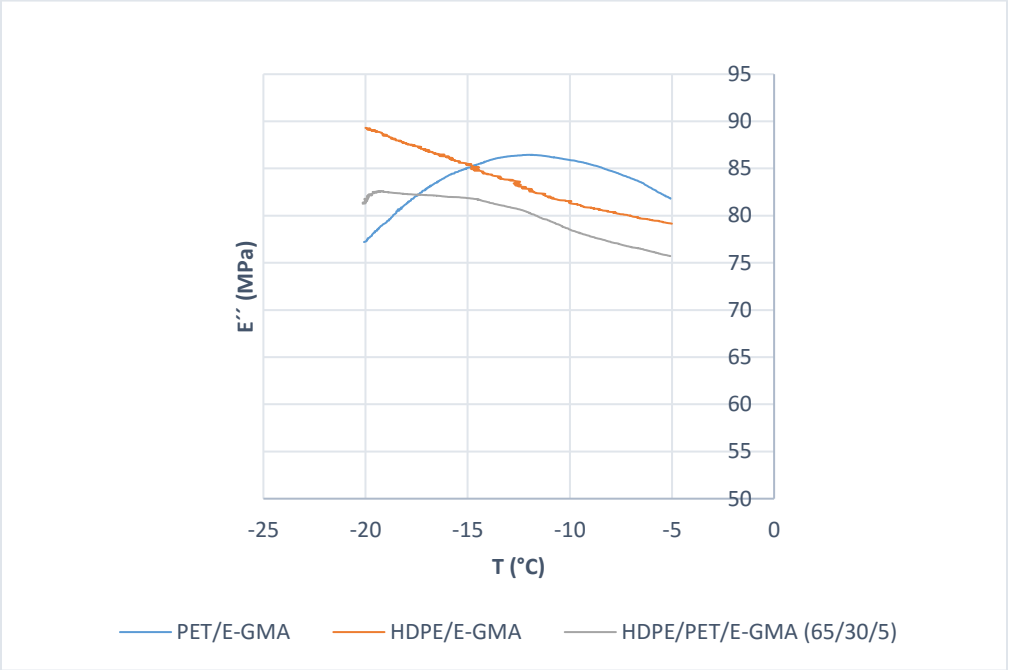

Table 5. Temperature at peak of E´´ in fig 7

Material	Temperature at peak (°C)
PET/E-GMA	-11.96
HDPE/E-GMA	N/A
HDPE/PET/E-GMA (65/30/5)	-19.27

2.5 Rotational rheometric analysis

According to equation 8, it is possible to estimate the interfacial tensions between two phases when it is known the characteristic relaxation time of blends shear oscillations and use this values in equations 1 and 2 to calculate the spreading coefficients and predict the morphology of ternary blends based on fig 1. Table 6 shows the characteristic relaxation times for HDPE/PET, HDPE/E-GMA and PET/E-GMA binary blends obtained by rotational rheometric tests. As it can be seen on figs 9 and 10, it was not possible to distinguish the E-GMA dispersed phase in the HDPE/E-GMA binary blend by any of the etching techniques proposed in this work, so this theoretical approach for predicting morphology could not be done. The failure in seeing a dispersed phase in the HDPE/E-GMA blend matches the high miscibility conjecture between HDPE and E-GMA.

Fig 9. HDPE/E-GMA (95/5) etched with n-heptane

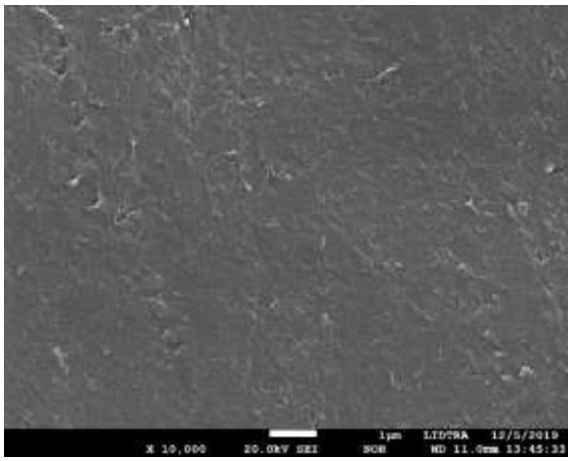

Fig 10. HDPE/E-GMA (95/5) etched with foron blue

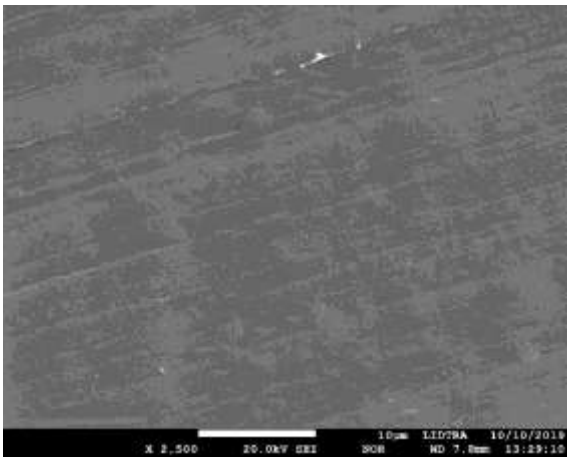

Table 6. Characteristic relaxation times on binary blends

Material	Characteristic relaxation time (s)
PET/E-GMA	5.74 E^{-2}
HDPE/E-GMA	1.06 E^{-1}
HDPE/PET	5.39 E^{-1}

Additional efforts were made in order to obtain the interfacial tension for binary blends by adjusting the experimental data of G´and G´´ to the proposed models in equations (3) to (8). No good correlation was obtained. At a closer inspection, equation (5) It is expressed in such a way that the value obtained for viscosity of the binary blend (η) will always be higher than the viscosity of the matrix (η_m), condition not shown by the experimental results obtained in this work. No reference values

were found in the literature for interfacial tension between HDPE/E-GMA and PET/E-GMA.

Fig 11. Viscosity curve of pristine materials and binary blends

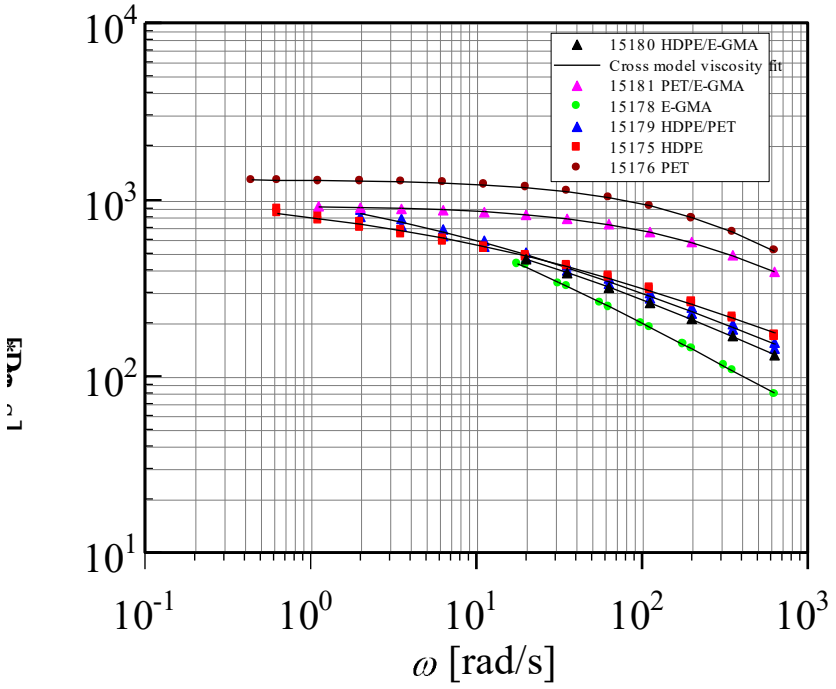

As can be seen on fig 11, the viscosity of HDPE remains virtually unaffected by the addition of PET and E-GMA at the given shear rate ratio. This shear rate ratio matches with the estimated one in the cavities of injection molded parts made in PTM, which indicates that processing these materials virtually will not affect the process parameters.

Fig 12. Effect of viscosity ratio on E, the ratio of viscous to interfacial forces required for drop burst in Couette shear

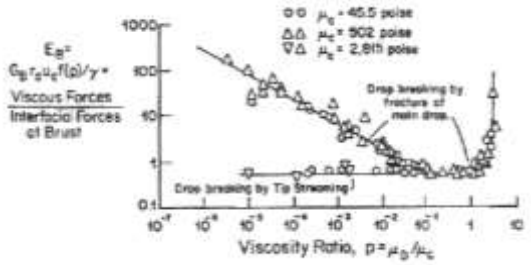

Fuente: Grace, 1982

Fig 11 also shows the effect of E-GMA on PET viscosity. As can be observed, the viscosity ratio between HDPE and PET gets closer to 1 taking advantage of this effect. Fig 12 was extracted from the original Grace´s work (Grace, 1982) about dispersion phenomena in high viscosity inmiscible fluid systems and represents the effect of viscosity ratio on the forces required for drop burst in shear flow. As can be deducted, a viscosity ratio closer to 1 facilitates dispersion of PET in HDPE even in single screw extruders or injection molding machines.

3. CONCLUSION

The morphology of HDPE/PET/E-GMA ternary blends showing toughening without rigidity loss was studied in this work as a response to the need for improve the mechanical properties of recycled materials in an upcycling context.

The impact strength of the HDPE/PET/E-GMA ternary blends improves while increasing the PET content, which is explained by the decrease in the interparticle distance of the homogenous dispersed phase observed in SEM micrographs. This phenomena, in conjunction with the increase in flexural properties, suggests a particular morphology in which the disperse phase acts as a rubbery one with a hard core that provides rigidity to the blend, a core-shell morphology. E-GMA also helps reducing the size of the dispersed phase of PET in the HDPE matrix, fact that can be observed in the SEM micrographs.

Three separated phases where found in the blend, another critical feature of core-shell morphologies, according to loss modulus measurements on DMA. DSC shows only two separated phases, HDPE and PET, but it is known that DMA is a more sensitive technique for phase transition observation. In addition, DSC shows that E-GMA does not act as a traditional compatibilizer shifting the transition temperature of the components towards each other, reinforcing the core-shell assumption.

The rotational rheometry test´s main objective was the theoretical demonstration of the morphology using Harkins equation, nevertheless it was not possible to estimate the interfacial tension in the binary blends because their behavior does not match the proposed by Gramespacher and Meissner based on the empirical rule of blending. An interesting observation made from the rheometry tests suggests that E-GMA reduces the viscosity of PET bringing it closer to that of HDPE and, according to Grace diagram, facilitating dispersion even in shear flow.

The morphology formation mechanism proposed in this work assumes that there is high miscibility of E-GMA on HDPE, for this reason E-GMA alone does not improve the impact strength of HDPE, but with the addition of PET the E-GMA surround the droplets of dispersed phase seeking to react and forms a core shell morphology.

4. REFERENCES

Bridgens, B., Powell, M., Farmer, G., Walsh, C., Reed, E., Royaporr, M., Gosling, P., Hall, H. & Heidrich, O. (2018). Creative upcycling: Reconnecting people, materials and place through making. J. Clean. Prod., 189, 145–154. Recuperado de https://doi.org/10.1016/j.jclepro.2018.03.317

Chen, F., Shangguan, Y., Jiang, Y., Qiu, B., Luo, G. & Zheng, Q. (2015). Toughening with little rigidity loss and mechanism for modified polypropylene by polymer particles with core-shell structure, Polymer, 65, 81–92. Recuperado de http://dx.doi.org/10.1016/j.polymer.2015.03.064

Grace, H. (1982). Dispersion phenomena in high viscosityimmiscible fluid systems and application of static mixers as dispersion devices in such systems. Chemical Engineering Communications, 14, 225-277. Recuperado de https://doi.org/10.1080/00986448208911047

Graebling, D., Muller, R. & Palierne, J. (1993). Linear viscoelastic behavior of some incompatible polymer blends in the melt. Interpretation of data with a model of emulsion of viscoelastic liquids, Macromolecules, 26, 320–329. Recuperado de https://doi.org/10.1021/ma00054a011

Hahladakis, J. & Iacovidou, E. (2019). An overview of the challenges and trade-offs in closing the loop of post-consumer plastic waste (PCPW): Focus on recycling, J. Hazard. Mater., 380, 120887. Recuperado de https://doi.org/10.1016/j.jhazmat.2019.120887

Jia, E., Zhao, S., Shangguan, Y. & Zheng, Q. (2019). Toughening mechanism of polypropylene bends with polymer particles in core-shell structure: Equivalent rubber content effect related to core-shell interfacial strength, Polymer, 178, 121602. Recuperado de https://doi.org/10.1016/j.polymer.2019.121602

Kalfoglou, N., Skafidas, D., Kallitsis, J., Lambert, J. & Van der Stappen, L. (1995) Comparison of compatibilizer effectiveness for PET/HDPE blends, Polymer, 36, 4453-4462. Recuperado de https://doi.org/10.1016/0032-3861(95)96853-Z

Khalili, R., Jafari, S., Saeb, M., Khonakdar, H., Wagenknecht, U. & Heinrich, G. (2014). Toward in situ compatibilization of polyolefin ternary blends through morphological manipulations, Macromol. Mater. Eng., 299, 1197–1212. Recuperado de https://doi.org/10.1002/mame.201300452

Lei, Y., Wu, Q. & Zhang, Q., (2009). Morphology and properties of microfibrillar composites based on recycled poly (ethylene terephthalate) and high density polyethylene, Compos. Part A Appl. Sci. Manuf., 40, 904–912. Recuperado de https://doi.org/10.1016/j.compositesa.2009.04.017

Luzinov, I., Pagnoulle, C. & Jérôme, R. (2000). Ternary polymer blend with core-shell dispersed phases: Effect of the core-forming polymer on phase morphology and mechanical properties, Polymer, 41, 7099–7109. Recuperado de https://doi.org/10.1016/S0032-3861(00)00057-4

Mi, D., Wang, Y., Kuzmanovic, M., Delva, L., Jiang, Y., Cardon, L., Zhang, J. & Ragaert, K. (2019) Effects of phase morphology on mechanical properties: Oriented/unoriented PP crystal combination with spherical/microfibrillar PET phase, Polymers (Basel) , 11, 248-263. Recuperado de https://doi.org/10.3390/polym11020248

Mwanza, B. & Mbohwa, C. (2017). Drivers to Sustainable Plastic Solid Waste Recycling: A Review, Procedia Manuf., 8, 649–656. Recuperado de https://doi.org/10.1016/j.promfg.2017.02.083

Palierne, J. (1990). Linear rheology of viscoelastic emulsions with interfacial tension, Rheol. Acta, 29, 204–214. Recuperado de https://doi.org/10.1007/BF01331356

Raheem, A., Noor, Z., Hassan, A., Abd Hamid, M., Samsudin, S. & Sabeen, A. (2019). Current developments in chemical recycling of post-consumer polyethylene terephthalate wastes for new materials production: A review, J. Clean. Prod., 225, 1052–1064. Recuperado de https://doi.org/10.1016/j.jclepro.2019.04.019

Salleh, M., Ahmad, S., Ghani, M. & Chen, R. (2013). Effect of compatibilizer on impact and morphological analysis of recycled HDPE/PET blends, AIP Conf. Proc., 1571, 70–74. Recuperado de http://dx.doi.org/10.1063/1.4858632

Scheirs, J. (2003). Modern Polyesters: Chemistry and Technology of Polyesters and Copolyesters. John Wiley & Sons, 495-539.

Shen, C., Zhou, Y., Dou, R., Wang, W., Yin, B. & Yang, M. (2015). Effect of the core-forming polymer on phase morphology and mechanical properties of PA6/EPDM-g-MA/HDPE ternary blends, Polymer, 56, 395–405. Recuperado de http://dx.doi.org/10.1016/j.polymer.2014.11.027

Tolinski, M. (2015). Additives for Polyolefins. Introduction. 3–7. William Andrew Publishing.

Wang, Y., Mi, D., Delva, L., Cardon, L., Zhang, J. & Ragaert, K. (2018). New approach to optimize mechanical properties of the immiscible polypropylene/poly(ethylene terephthalate) blend: Effect of shish-kebab and core-shell structure, Polymers (Basel)., 10, 1094-1110. Recuperado de https://doi.org/10.3390/polym10101094